

Article

Effect of Physical Properties and Chemical Substitution of Excipient on Compaction and Disintegration Behavior of Tablet: A Case Study of Low-Substituted Hydroxypropyl Cellulose (L-HPC)

Saurabh M Mishra ^{1,*}  and Andreas Sauer ²¹ SE Tylose USA Inc., Pharmaceutical Application Laboratory, Totowa, NJ 07512, USA² SE Tylose GmbH & Co., KG, Kasteler Str. 45, 65203 Wiesbaden, Germany; andreas.sauer@setylose.com

* Correspondence: saurabh.mishra@setyloseusa.com; Tel.: +1-973-837-8001

Abstract: As final attributes of dosage form largely depend on the properties of excipients used, understanding the effect of physicochemical properties of excipients is important. In the present study, six grades of L-HPC with varying degrees of particle size and hydroxypropyl content and the influence of the grade on compaction as well as disintegration behavior were studied. All grades of L-HPC were compressed at different compression loads to achieve different tablet porosity. Compressibility and compactibility of L-HPC grades were evaluated using a modified Heckel equation and percolation model. Further effects of particle size and hydroxypropyl content of L-HPC on tablet porosity and disintegration time were evaluated using a 3² full-factorial design. From compaction studies, it was found that compressibility of L-HPC largely depends upon the particle size with lower particle size grade showing lower compressibility. Whereas consolidation/bonding behavior of L-HPC is independent of particle size and % hydroxypropyl content. By factorial design, it was found that particle size and % hydroxypropyl content have a significant effect on the disintegration behavior of L-HPC. It was found that smaller particle sizes and higher hydroxypropyl content of L-HPC show longer disintegration time. Thus, careful consideration of excipients selection should be made to achieve desired quality attribute of the product.

Keywords: L-HPC; low-substituted hydroxypropyl cellulose; excipient: compressibility; compactibility; disintegration; particle size; hydroxypropyl substitution; 3² full-factorial design; percolation theory



Citation: Mishra, S.M.; Sauer, A. Effect of Physical Properties and Chemical Substitution of Excipient on Compaction and Disintegration Behavior of Tablet: A Case Study of Low-Substituted Hydroxypropyl Cellulose (L-HPC). *Macromol* **2022**, *2*, 113–130. <https://doi.org/10.3390/macromol2010007>

Academic Editor: Ana María Díez-Pascual

Received: 5 January 2022

Accepted: 8 February 2022

Published: 4 March 2022

Publisher's Note: MDPI stays neutral with regard to jurisdictional claims in published maps and institutional affiliations.



Copyright: © 2022 by the authors. Licensee MDPI, Basel, Switzerland. This article is an open access article distributed under the terms and conditions of the Creative Commons Attribution (CC BY) license (<https://creativecommons.org/licenses/by/4.0/>).

1. Introduction

Pharmaceutical excipients are an inert material with no therapeutic or pharmacological effect. However, the performance of drug/API to be delivered at the desired site, desired rate, and desired amount largely depend upon the properties of these excipients [1]. However, the source of excipients is wide, including plant, animal, mineral, biotechnology, and chemical synthesis. Additionally, polymeric excipients differ in their physical properties such as particle size, morphology, polymorphic forms as well as cross-linkages, molecular weights, and molar substitution ratio from different sources or suppliers of these excipients [1]. These excipient variabilities may have large influences on their functionality and performance in the dosage form. It has also been reported that the same excipients with different particle sizes or polymorphic forms can have different applications [2–4]. Microcrystalline cellulose (MCC) is available in various particle sizes with approximately the same degree of polymerization, polymorphic form, and moisture content. However, the application of MCC differs within different grades due to differences in particle size; for instance, MCC PH101 (D₅₀ = 50 μm) is widely used in wet granulation, whereas MCC PH102 (D₅₀ = 100 μm) is widely used for direct compression [3,4]. On the same line, MCC is also available in different polymorphic forms with a low degree of crystallinity,

Cellulose II (47–57%) showing lower compactibility and rapid disintegration in comparison with highly crystalline MCC, Cellulose I (77%) [5,6]. Similarly, it has been reported that the compaction behavior of lactose monohydrate varies with small variations in hydrate form, moisture content, and particle size [7,8]. Hence, it is important for a formulation scientist to understand that slight variability in different grades of an excipient can cause a larger deviation in the intended use of the same excipients. Thus, in the present study, an attempt has been made to understand the effect of different grades of Low-substituted hydroxypropyl cellulose (L-HPC), a multifunctional novel excipient commonly used as a binder and disintegrant on compaction as well as its disintegration behavior [9].

L-HPC is low-substituted hydroxypropyl cellulose with a molar substitution of 0.2 (average number of hydroxypropyl groups per glucose unit) compared to hydroxypropyl cellulose (HPC) with molar substitution of 3.5 (Figure 1).

Due to low molar substitution, L-HPC is water-insoluble compared to HPC, which is highly water-soluble and shows high swelling, due to which L-HPC can act as a very effective disintegrant [10]. It was first introduced in Japan in 1977. Over time, nine grades of L-HPC have been introduced in the market. The grades of L-HPC are broadly classified based on differences in particle size as well as % of hydroxypropyl (HPO) content. An evaluation of literature reveals various reports on the application of L-HPC and its grades as a filler, binder, or disintegrant in developing solid dosage forms. However, detailed studies of compaction and disintegration behavior of pure L-HPC and its grades are limited. Recently, ElShaer et al. [11] reported the effect of different grades of L-HPC grades on its compaction and disintegration behavior. However, the study was limited to only four grades of L-HPC (LH-11, LH-21, LH-B1, and LH-32) with LH-11, LH-21, and LH-B1 having a similar particle size of approximately 45–50 μm and similar hydroxypropyl (HPO) content of 11%. Among the four grades, only LH-32 had a different particle size (20 μm) and HPO content of 8%. Moreover, the results of compressibility of L-HPC grades from the Heckel equation were reported by authors to be very high; 2000 MPa, 625 MPa, 434.78 MPa, 769.23 MPa for LH-32, LH-11, LH-21, and LH-B1, respectively. Similarly, very high compactibility (tensile strength at zero porosity, σ_0) were reported for LH-32 (108.68 MPa), LH-11 (9171.50 MPa), LH-21 (1120.30 MPa), and LH-B1 (5081.40 MPa) by exponential equation. The observed compressibility and compactibility are very high and uncommon for pharmaceutical powders, especially L-HPC being a plastic binder/disintegrant [12,13]. This could be attributed to the error in the estimation of the true density value of L-HPC grades by ElShaer et al. [11], which was reported to be more than 2.5 g/cm^3 , significantly higher than the reported value by Alvarez-Lorenzo et al. (1.43–1.45 g/cm^3) [14] and Schaller et al. (1.46–1.48 g/cm^3) [15]. Moreover, a true density value of 1.3 g/cm^3 of all L-HPC grades has also been reported in the manufacturer's technical literature (Shin-Etsu Chemicals Co, Ltd., Tokyo, Japan) [16]. This confirms that true density values of L-HPC grades reported by ElShaer et al. [11] ($>2.5 \text{ g}/\text{cm}^3$) were too high, thus leading to overestimation of compressibility and compactibility of L-HPC grades [17,18]. Hence, a precise and accurate calculation of compressibility and compactibility of different L-HPC grades based on established mathematical models as well as powder technology rules was required. To achieve this, six different grades of L-HPC with three different particle sizes but the same %HPO content (LH-11, LH-21, LH-31) and L-HPC grade having the same particle size but different %HPO content (NBD-020, NBD-021, NBD-022) was selected (Table 1). Thus, a broad spectrum to study the effect of particle size and hydroxypropyl (HPO) content on compaction and disintegration behavior of L-HPC grades was carried out, which has not been performed before based on our best knowledge. To study the compaction behavior of L-HPC grades, compressibility and compactibility have been calculated using a modified Heckel equation as well as percolation model of powder compaction, whereas to study the disintegration behavior of L-HPC grades, quality by design approach using 3^2 full-factorial design has been used.

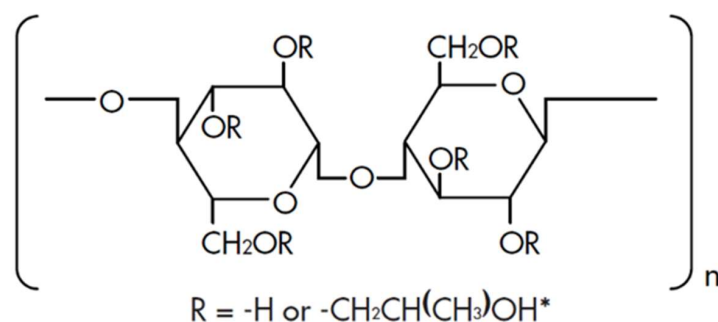


Figure 1. Molecular structure of L-HPC—Reproduced with permission from Shin-Etsu Chemical Co. Ltd (Tokyo, Japan) (www.metolose.jp) [16].

Table 1. Particle size and % hydroxypropyl (HPO) content of different L-HPC grades.

Grade	Particle Size (D50) (μm)	HPO Content (%)
LH-11	52	10.8
LH-21	49.8	11
LH-31	19.4	11.3
NBD-020	42.3	13.8
NBD-021	39.6	10.9
NBD-022	38.7	8.2

All values are reported from the Certificate of Analysis of manufacturer Shin-Etsu Chemical Co. Ltd. (Tokyo, Japan).

2. Materials and Methods

2.1. Materials

All six grades of L-HPC (LH-11, LH-21, LH-31, NBD-020, NBD-021, NBD-022) were received from Shin-Etsu Chemical Co. Ltd. (Tokyo, Japan). All other reagents used in this study was of analytical grade.

2.2. Methods

2.2.1. Physical Characterization of Powder Materials

True density: True density of the powder materials was determined using a gas pycnometer (AccuPyc[®] II 1340, Micromeritics Instruments Corp., Norcross, GA, USA). The determinations were carried out at room temperature by repeating the sample density for up to 10 cycles. The average reading of 10 cycles was recorded as the true density of the material [19].

Bulk and tapped densities: Bulk density of powder materials was determined by placing a known quantity of pre-sieved powder material into a graduated cylinder and recording the occupied volume. The bulk density of the powder material was computed from the mass and volume of the powder. Tapped density was determined by placing the same graduated cylinder on a Caleva Tap Density Tester (Type TD2, Dorset England), which was operated for a fixed number of taps (300 taps) to attain equilibrium in powder bed volume. The tapped density was computed from the mass and tapped volume of the powder [20].

Morphological characteristics: Morphological analysis of different grades of L-HPC was carried out using Scanning Electronic Microscopy (SEM) TM3000 (Hitachi, Tokyo, Japan). The samples were observed on SEM operating at an accelerating voltage of 15 KV under analysis mode at a magnification of $\times 200$.

2.2.2. Compression of Powders and Evaluation of Tablet Properties

Compression of L-HPC Powder Materials: Powder materials were compressed using a set of 10 mm, flat-faced tooling (Natoli Engineering Co. Inc., St. Charles, MO, USA) using Hand tap-200 (Ichihashi Seiki, Kyoto, Japan) at various compression loads

($n = 6$ per compression pressure) to obtain compacts of a wide range of relative density (tablet porosity).

Relative density and porosity: Relative density, ρ_r , of tablets compressed at various pressures was calculated from compact density data and true density of powder using the following relationship (Equation (1)) [21].

$$\rho_r = \frac{\text{Compact density}}{\text{True density of the powder}} \quad (1)$$

The porosity of the tablet, ε , can be calculated with the following relationship [21].

$$\varepsilon = 1 - \rho_r \quad (2)$$

Radial tensile strength: Radial tensile strength, σ_t , of tablets was determined from tablet crushing strength and tablet dimension data using the following equation (Equation (3)) [22].

$$\sigma_t = \frac{2F}{\pi \cdot d \cdot h} \quad (3)$$

where F is the tablet crushing force (N), d is the diameter (mm), and h is the thickness (mm) of the tablet. Crushing force of tablets along with diameter and thickness was determined using an Erweka hardness tester (TB125, Erweka GmbH, Langen, Germany).

Disintegration test of tablets: The disintegration time of tablets was determined using a disintegration apparatus (ZT72, Erweka GmbH, Langen, Germany) as per USP specifications. Disintegration test was carried out using 900 mL of purified water maintained at 37 ± 0.5 °C. The tablet was supposed to have disintegrated when all powder particles passed through the 10-mesh screen after tablet disintegration. Each determination was carried out on 1 tablet at a time and was conducted on 6 tablets. The disintegration time of the tablets was recorded, and the mean of these determinations with the corresponding standard deviation was computed.

2.2.3. Evaluation of Swelling Pressure and Water Absorption of L-HPC Powder

To measure swelling pressure of L-HPC powder materials, 1 g of powder sample was prepared and swelling force generated in presence of water was measured with a 25 mm probe with the application of 0.2 N force to test the speed of 1 mm/s using a texture analyzer (TA-XT Plus) (Stable Microsystems, Godalming, England). Water absorption by L-HPC powder was measured according to Zhao and Augsburg [23] using 1 g of powder sample in presence of water (Syringe: $\varnothing 15$ mm, 10 mL, Burette: 10 mL). The amount of water absorbed was visually measured over time until the sample completely absorbed water. For evaluating swelling pressure and water absorption, three measurements ($n = 3$) of each L-HPC grade powder sample were made.

2.2.4. Estimation of Compressibility and Compactibility Parameters

In powder technology, compression of powder is usually defined in terms of compressibility and compactibility [24]. The term compressibility can be defined as the ability of a powder material to decrease in volume under pressure, and compactibility can be defined as the ability of powder material to be compressed into tablets of specific strength [24,25]. Thus, these two properties govern the ability of powder material for the successful formation of a tablet.

Compressibility of L-HPC Grades Powder Materials

Among various theories to define compressibility or volume reduction of powder with the application of compression load, the Heckel equation is still the most popular (Equation (4)) [26].

$$\ln\left(\frac{1}{1 - \rho_r}\right) = k \sigma_c + a \quad (4)$$

where ρ_r and σ_c are relative density and compression pressure, respectively, and k and a are constants derived from the slope and intercept of the straight line, respectively, of the Heckel plot. The mean yield pressure or compressibility of powder materials is determined from slope, k , of the Heckel plot. However, as the slope value, k , in the Heckel plot depends on both the fragmentation and the elastic/plastic deformation of the material, the value of mean yield pressure achieved can be incorrect and thus deceptive in characterizing deformation or compressibility of powder material [13,27]. In the present study, therefore, the compressibility of L-HPC grades of powder materials was determined from the modified Heckel equation, which was found to be more accurate to determine compressibility/deformation behavior of powder materials (Equation (5)) [28]. This could be attributed to the fact that the modified Heckel equation considers critical relative density, which allows the calculation of critical relative density or porosity for pore elimination in powders during the compaction phenomenon (Equation (5)) [27].

$$\sigma_c = \frac{1}{C} \left[\rho_c - \rho_r - (1 - \rho_c) \ln \left(\frac{1 - \rho_r}{1 - \rho_c} \right) \right] \quad (5)$$

where σ_c , and ρ_r are compression load and relative density of compact, respectively. The term C in Equation (5) represents compressibility parameters of powder materials, and its inverse form ($1/C$) depicts the compressibility of powder materials or mean yield pressure value; ρ_c is a percolation threshold defining critical relative density at which pressure susceptibility of powder materials changes and 3-dimensional structures is formed in powder materials. Thus, powder materials with a lower value of $1/C$ and ρ_c are more susceptible to pressure and thus highly compressible [27,28].

Compactibility of L-HPC Grades Powder Materials

Similar to determining the compressibility of material, numerous equations have been proposed to quantify the compactibility of material. Amongst them, the Leuenberger equation [24] and the Ryshkewitch Duckworth equation [29] are two of the most widely accepted models to quantify the compactibility of material. In the previous study, it was found that both equations have limited application in the case of disordered pharmaceutical powder materials and thus are not able to quantify the compactibility of powder materials satisfactorily [13]. Thus, the percolation model, a mathematical relationship based on percolation theory, has been used to study the compactibility of various grades of L-HPC by plotting tensile strength vs. relative density (Equation (6)) [13,30]. The detailed theoretical description of this model can be found elsewhere [13,31].

$$\sigma_t = \sigma_0 \left(\frac{\rho_r - \rho_c}{1 - \rho_c} \right)^q \quad (6)$$

where σ_t is the tensile strength of compacts, σ_0 is the tensile strength of compact at zero porosity, ρ_r is the relative density of the compact, ρ_c is percolation threshold, and q is the critical exponent. The normalization of the relative density of compact can be done by substituting the known value of the percolation threshold directly into Equation (6) [32]. However, in the present study, the relative density of compact was normalized directly by assuming the value of the critical exponent, $q = 2.7$ [30,31,33]. One of the advantages of using this approach is the elimination of the flip-flop effect between adjusting functions, q and ρ_c , of the power law equation [34].

2.2.5. Non-Linear Regression Analysis and Statistical Evaluation

Compressibility and compactibility parameters using Equations (5) and (6) were calculated using Origin Pro (Origin Labs Corporation, Northampton, MA, USA). To evaluate dispersion or variability of model parameters at 95 % confidence interval, values of all model parameters are reported, along with the standard error of fitting. Among various statistical parameters, to assess the efficiency of the model, the values of the coefficient of

determination (R^2) are widely used. Although an indicator of how well the data fit in the model, this parameter usually fails to demonstrate the superiority of one model over the other when analyzing the same set of data [35]. Thus, other than R^2 values, adjusted R^2 values, as well as the root mean square error values (RMSE), were also used as statistical parameters to evaluate the efficiency of all models used in the present study.

2.2.6. Effect of Different L-HPC Grades on Porosity and Disintegration Time Using 3^2 Full-Factorial Design

To study the impact of independent variables such as compression load as well as physical properties and chemical substitution such as particle size and %HPO content on porosity and disintegration time of tablets, a 3^2 full-factorial design was used as a tool to design the experiment. As the physical and chemical substitution variables of grades such as particle size and %HPO content cannot be studied together (Table 1), due to the limitation of statistical design, two separate 3^2 factorial designs were created. In the first 3^2 full-factorial design matrix, three different levels of applied compression load and particle size of three different L-HPC grades (LH-11, LH-21, and LH-31) were used, whereas in the second 3^2 full-factorial design matrix, three levels of compression load and %HPO content of three different grades of L-HPC (NBD-020, NBD-021, NBD-022) were used (Table 2). Each of the two 3^2 full-factorial design matrixes consists of 9 experimental runs, and their effect on porosity as well as disintegration time of L-HPC compacts was evaluated. The value of particle size (D50) and %HPO content in the present study was obtained from the CoA provided by the manufacturer. The independent factors were prescribed into three levels ($-1, 0, +1$) as low, medium, and high, respectively (Table 2). The design of experiments (DoE) was constructed using commercially available software (JMP 12, SAS[®] Institute Inc., Cary, NC, USA). The relationship between independent variables with the responses was quantified using Equation (7) [36].

$$Y = B_0 + B_1X_1 + B_2X_2 + B_{12}X_1X_2 \quad (7)$$

where Y is the predicted or measured response, B_0 is model constant or intercept, X_1 and X_2 are independent variables, B_1 and B_2 are linear coefficients, and B_{12} is interaction terms between independent variables or cross product coefficients [37]. The effect of the independent variable was evaluated by multiple regression analysis and ANOVA at a 95% confidence interval ($p < 0.05$).

Table 2. Experimental Design Matrix- 3^2 full-factorial design. Value of particle size and %HPO content was used from COA.

Design I: Effect of Particle Size and Compression Load on Tablet Porosity and Disintegration Time			
Independent Variables	Level		
	Low (-1)	Medium (0)	High (+1)
Particle size (μm)	19.4 (LH-31)	49.8 (LH-21)	52 (LH-11)
Compression load (MPa)	25	50	75
Design II: Effect of % HPO Content and Compression Load on Tablet Porosity and Disintegration Time			
Independent Variables	Level		
	Low (-1)	Medium (0)	High (+1)
Hydroxypropyl content (%)	8.2 (NBD-022)	10.9 (NBD-021)	13.8 (NBD-020)
Compression load (MPa)	25	50	75
Responses			
Tablet Porosity (%)			
Disintegration time (s)			

3. Results and Discussion

3.1. Physicochemical and Morphological Properties of L-HPC Grades

Bulk tapped and true density of all L-HPC grades are summarized in Table 3. Among all the physicochemical properties of the powder, true density is one of the most important fundamental properties of powder as it is used to estimate tablet relative density (Equation (1)) and tablet porosity (Equation (2)). As relative density and tablet porosity are eventually used to estimate compressibility (Equation (5)) and compactibility of powder materials (Equation (6)), true density is a critical material attribute of powder materials. Thus, a careful determination of true density should be made to avoid overestimation of powder compaction data such as compressibility and compactibility [17,18]. As observed from Table 3, the true density of all L-HPC grades is less than 1.5 g/cm^3 . This is contrary to ElShaer et al. [11], who reported a true density value of L-HPC more than $>2.5 \text{ g/cm}^3$. Moreover, a similar true density value range ($1.39\text{--}1.48 \text{ g/cm}^3$) of different grades of L-HPC has been reported by previously mentioned authors Alvarez-Lorenzo et al. ($1.43\text{--}1.45 \text{ g/cm}^3$ [14] and Schaller et al. ($1.46\text{--}1.48 \text{ g/cm}^3$) [15], as well as by the manufacturer [16]. Thus, additional validity of robustness for reported true density values as well as estimation of compressibility and compactibility of L-HPC grades were achieved in the present study.

Table 3. Physical properties of L-HPC grades.

Grades	Bulk Density (g/cm^3)	Tapped Density (g/cm^3)	True Density (g/cm^3)
LH-11	0.314 ± 0.020	0.489 ± 0.030	1.3955 ± 0.0007
LH-21	0.375 ± 0.022	0.618 ± 0.034	1.4446 ± 0.0004
LH-31	0.295 ± 0.018	0.519 ± 0.029	1.4252 ± 0.0003
NBD-020	0.317 ± 0.014	0.491 ± 0.021	1.4466 ± 0.0004
NBD-021	0.310 ± 0.019	0.480 ± 0.021	1.3948 ± 0.0007
NBD-022	0.313 ± 0.015	0.491 ± 0.024	1.4768 ± 0.0012

To study the morphological characteristics of L-HPC grades, SEM analysis was carried out. Based on Figure 2, it can be observed that among all six grades of L-HPC, LH-11 was found to be mostly fibrous in nature, showing long fiber-like particles, whereas in the case of LH-21 and LH-31, the fibrous content was smaller than LH-11 with LH-31 showing smallest particle size. Among NBD grades (NBD-020, NBD-021, NBD-022) all three grades show short particles with the absence of fiber-like particles. No pronounced difference in morphological nature among all three NBD grades was found from SEM images.

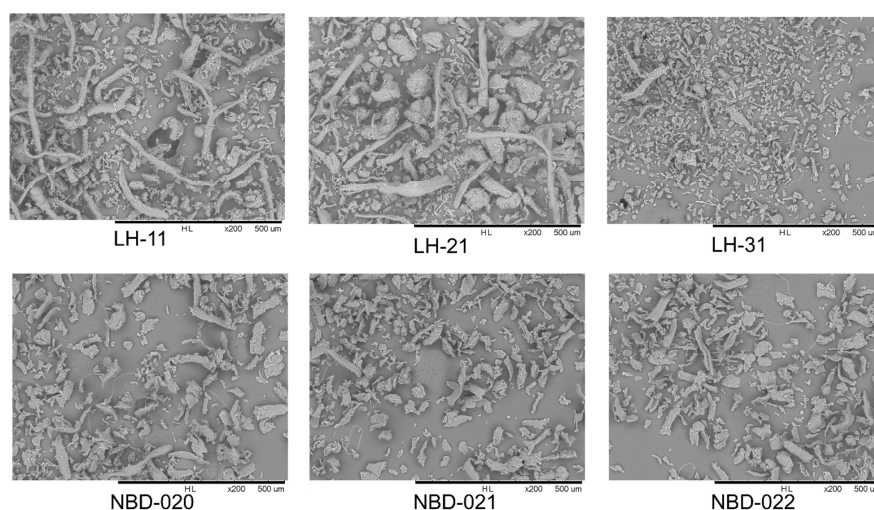


Figure 2. Morphological analysis of all six grades of L-HPC powder using scanning electron microscope (SEM) at $\times 200$ magnification.

3.2. Compressibility of Different Grades of L-HPC

Most of the active pharmaceutical ingredients (APIs) inherently have poor flow and compression properties that pose a major challenge for direct compression, especially in the case of high-dose drugs. For this purpose, various directly compressible excipients such as diluent and binder are used to compensate for these poor API properties, but this often limits the amount of API to 30% of the formulation [38]. Binders are the most critical excipient, as they must provide the required plasticity as well as bonding efficiency to the formulation. Plastic deformability is one of the most important aspects of binder functionality [39]. The addition of a binder enhances the bonding area and bonding strength of the formulation due to the change in surface properties. As the bonding area and bonding strength largely depend upon the degree of compressibility (plastic deformation) and compactibility of powder materials, higher compressibility and compactibility are some of the ideal characteristics of binders for direct compression [40].

In the present study, to elucidate the impact of compression load on all six L-HPC grades of powders, the surface morphology of different grades of L-HPC tablets compacted at 90 MPa has been illustrated by SEM (Figure 3). As observed in Figure 3, among L-HPC grades, differences in microstructure of tablets can be seen, especially in the case of LH-11, LH-21, and LH-31, due to differences in particle size as well as morphological characteristics. In the case of LH-11 tablets, fibrous particles can be identified on the tablet surface forming mechanical interlocking due to the application of the compression load [41]. The surface morphology of the LH-21 tablet also shows a smaller number of interlocked fibrous particles, whereas in the case of LH-31, a well-compacted structure with no void spaces can be observed owing to its smaller particle size. This result is consistent with the SEM images of original powder materials (Figure 2). No pronounced differences in the tablet morphology could be observed in the case of NBD grades NBD-020, NBD-021, and NBD-022 with different %HPO content with all three grades showing well-compacted structures. Thus, from SEM images, differences in morphological characteristics of the compacted tablet can be observed, especially in the case of different particle size grades of L-HPC and not in the case of grades having different %HPO content. Moreover, a well-consolidated and deformed particle structure for all L-HPC grades can be observed by SEM image (Figure 3). As compression of powder is a complex phenomenon with a large number of factors affecting it, it often needs to be analyzed by proper compression mathematical models [42,43]. For a definite understanding and quantitative determination of compressibility or deformation behavior of each L-HPC grades of powder, a modified Heckel equation (Equation (5)) has been used in the present study. The modified Heckel equation gives the most accurate analysis of compressibility/deformation behavior of powder because of its consideration of the fact that the rate constant for pore elimination varied with porosity of powder bed. Additionally, the modified Heckel equation considers the fact that there is the existence of critical porosity or critical relative density, a point where a three-dimensional structure is formed in the tablet [27,28]. The application of the modified Heckel equation in calculating critical porosity/relative density of powder along with compressibility parameters makes it more suitable to analyze and differentiate the compressibility of powders of different deformation behavior. In the present study, the compressibility/deformation behavior of all L-HPC grades of powders was evaluated with a modified Heckel equation (Equation (5)) by plotting compression pressure vs. relative density (Figure 4). Compressibility of powder ($1/C$) and percolation threshold, ρ_c , which indicates the critical relative density of powder to form 3-dimensional structure in the tablet was calculated from Equation (5) by nonlinear regression analysis.

The data for compressibility parameters, $1/C$ (MPa), and percolation threshold, ρ_c , along with fitting parameters of all six grades of L-HPC, are summarized in Table 4. Among different grades of L-HPC, NBD-021 shows the highest compressibility (low $1/C$ value, $1/C = 98.52 \pm 4.45$) followed by LH-11 (152.21 ± 6.55), LH-21 (172.12 ± 32.88), NBD-022 (176.99 ± 9.29), NBD-020 (188.68 ± 13.76), and LH-31 (204.92 ± 14.03). Moreover, the percolation threshold, ρ_c , the critical relative density at which the pressure susceptibility or

deformation behavior of powder changes and 3D structure is formed, was lowest in the case of NBD-021 (0.170 ± 0.017) and highest for LH-31 (0.292 ± 0.018) (Table 4). This demonstrates that NBD-021 is the most compressible grade of L-HPC, and LH-31 is the least compressible. The higher compressibility of NBD-021 could be attributed to a high degree of homogeneity of particle size and [44]. In contrast, the lower compressibility of LH-31 compared to other L-HPC grades can be attributed to its smaller particle size ($D_{50} = 19.4 \mu\text{m}$, Table 1), due to which resistance of powder particles undergoing deformation is larger. Roberts and Rowe [45] also reported that a decrease in particle size causes a decrease in strain rate sensitivity and thus an increase in yield pressure for permanent deformation. Hence, the powder with a lower particle size shows lower compressibility. A higher value of the percolation threshold, ρ_c , obtained for LH-31 also confirms that LH-31 is less compressible, since high relative density is required to cause a permanent deformation and form a mechanical stable compact compared to other grades of L-HPC. Thus, from the above study, it can be concluded that the compressibility or deformation mechanism of L-HPC grades depends upon the particle size. However, no correlation between compressibility parameters with %HPO content of L-HPC grades was found in the present study. As observed from the fitting of data in Table 4 using the modified Heckel equation, a low standard error of fitting and a high coefficient of determination (R^2) and adjusted R^2 values along with low root mean square error values (RMSE) values were achieved, thus confirming the robustness of the model for the estimation of compressibility of all L-HPC grades in the present study.

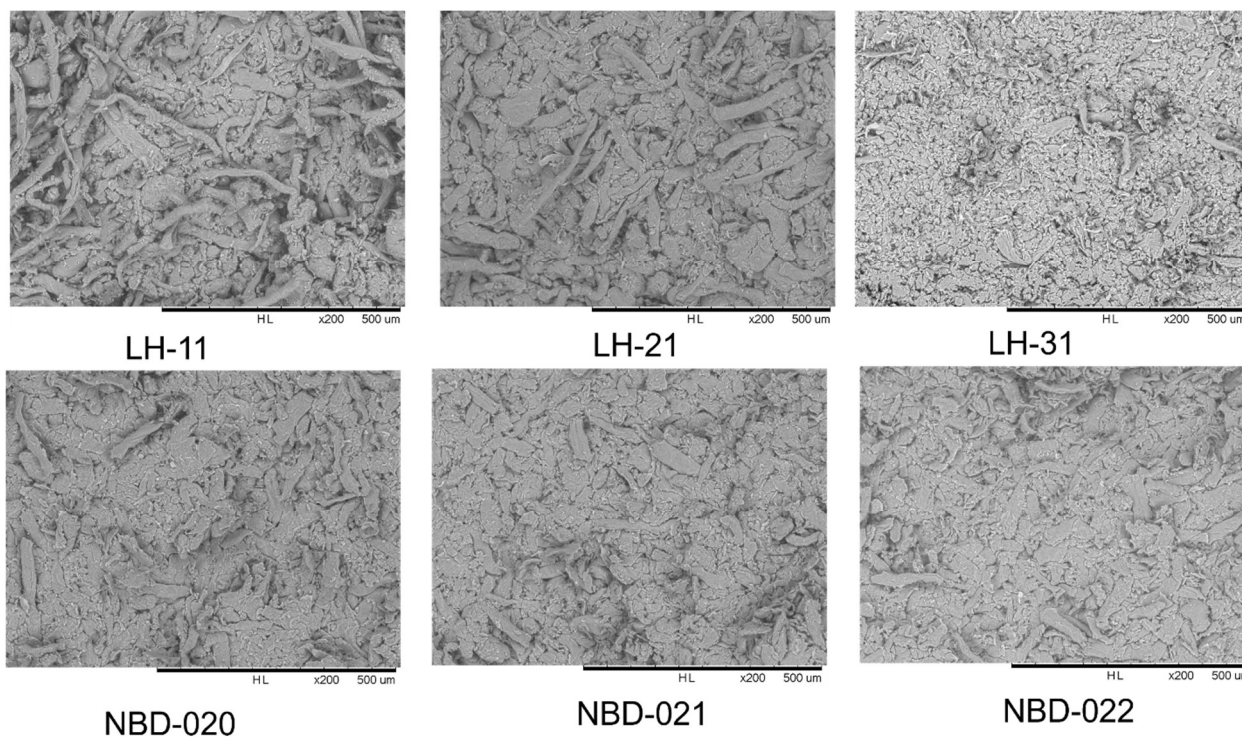


Figure 3. SEM images of L-HPC grades tablet compacted at 90 MPa at $\times 200$ magnification.

As mentioned above, the literature dealing with compaction behavior study of L-HPC and its grades is limited. The compressibility parameters of L-HPC grades calculated by a modified Heckel equation (Equation (5)) were compared with earlier reported data of microcrystalline cellulose (MCC PH 102) [46]. The compressibility parameters of MCC PH 102 by modified Heckel equation were found to be $C = 5.8 \pm 0.27 \times 10^{-3} \text{ MPa}^{-1}$ ($1/C = 172.41 \pm 8.02 \text{ MPa}$), and the percolation threshold $\rho_c = 0.198 \pm 0.011$ [46]. A comparative evaluation between compressibility parameters of L-HPC grades with reported values of MCC PH 102 reveals that NBD-021 and LH-11 are more compressible than microcrystalline cellulose with lower $1/C$ values. It is also worth mentioning that compressibility

parameters of LH-21 (172.12 ± 32.88) were similar to MCC PH 102, and compressibility/plasticity of other L-HPC grades (NBD-020, NBD-022) was approximately equivalent to the values of MCC PH 102 except LH-31. Additionally, an almost equivalent value of percolation threshold, ρ_c , of L-HPC grades with MCC PH 102 indicates that critical relative density to form a 3-D infinite cluster is similar for L-HPC grades and MCC PH 102 [27]. Thus, it can be concluded that L-HPC is more compressible (NBD-021, LH-11) or equivalent to some extent with MCC PH 102, a well-known established popular diluent that undergoes a high degree of plastic deformation [3].

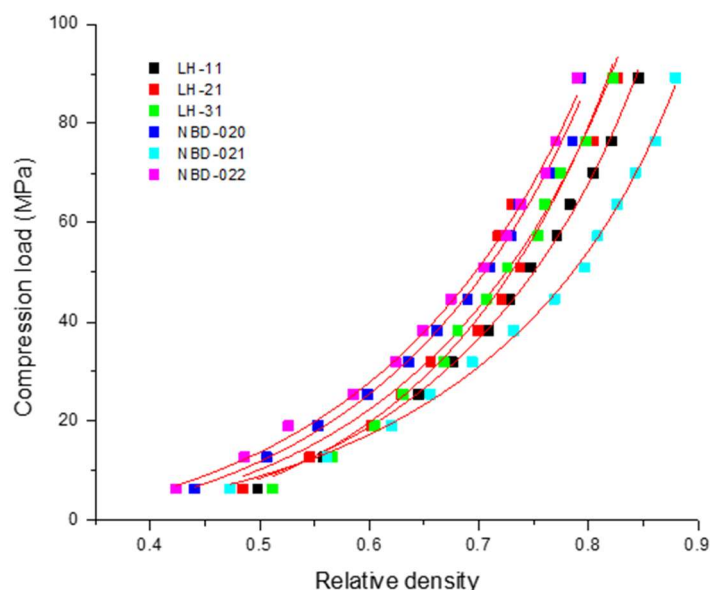


Figure 4. Plot depicting compression load vs. relative density of L-HPC grades as per modified Heckel equation (Equation (5)). The results of fitting parameters by nonlinear regression analysis are summarized in Table 4.

Table 4. Value of compressibility parameter and percolation threshold of L-HPC grades calculated by modified Heckel equation (Equation (5)). All values are reported as parameters \pm standard error of fit.

L-HPC Grade	Compressibility (1/C) (MPa)	Percolation Threshold (ρ_c) (-)	R ²	Adjusted R ²	Root Mean Square Error (RMSE)
LH-11	152.21 \pm 6.55	0.246 \pm 0.013	0.9975	0.9973	1.35
LH-21	172.12 \pm 32.88	0.237 \pm 0.057	0.9486	0.9439	6.08
LH-31	204.92 \pm 14.03	0.292 \pm 0.018	0.9931	0.9925	2.22
NBD-020	188.68 \pm 13.76	0.229 \pm 0.021	0.9928	0.9922	2.27
NBD-021	98.52 \pm 4.45	0.170 \pm 0.017	0.9976	0.9973	1.32
NBD-022	176.99 \pm 9.29	0.196 \pm 0.016	0.9963	0.9960	1.63

3.3. Compactibility of Different Grades of L-HPC

When particles are filled in a tablet die, powder particles rearrange themselves depending on the bulk density, particle size distributions, and other micrometric properties. Further, with the application of compression load, deformation or possibly fragmentation of particles occurs during compaction. The degree or sequence of these events depends largely upon the physicochemical and mechanical properties of powder materials [47]. With the application of stress, the powder particles come closer, and this results in the consolidation of the particles. The degree of consolidation of powder particles depends upon the compression pressure applied, as well as the particle–particle interactions [48]. For a description of the compactibility of powder materials, σ_0 , the tensile strength at zero porosity, is the most popular way to study the degree of consolidation of powder particles [49]. It has been

reported that the process of powder particles undergoing plastic deformation creates a large surface area and thus great bonding strength [40]. From the above study, L-HPC has been found to be highly compressible, undergoing predominately plastic deformation, and thus a high degree of consolidation/compactibility can be expected from L-HPC powder particles [40]. The percolation model was used to study the compactibility of L-HPC due to its higher accuracy, as discussed before, by plotting tensile strength, σ_0 , vs. relative density of compact, ρ_r . (Figure 5) [13]. The compactibility, σ_0 , of all six L-HPC grades and percolation threshold for compactibility, ρ_c , along with fitting parameters, have been summarized in Table 5. The manufacturing classification system group of Leane et al. reported that powder compactibility at a relative density of 0.85 (porosity of 0.15) and with tensile strength of 1.7 MPa is an acceptable candidate for direct compression [50]. Another study suggests that powders with compactibility, i.e., tensile strength at zero porosity, σ_0 , more than 5 Mpa, are highly compactible materials [51]. As evident in Table 5, the compactibility of all six grades of L-HPC is approximately equivalent to $\sigma_0 \sim 10$ MPa, thus indicating that the six grades of L-HPC tested are highly compactible materials. One of the few hypothetical reasons that the high degree of consolidation/compactibility of L-HPC could be attributed to is the presence of abundant hydrogen bonds enhancing particle–particle interactions as well as fibrous particles forming mechanical interlocks between particles [43,52]. This is also evident from the SEM images of different grades of L-HPC tablets (Figure 3) showing a well-consolidated but deformed structure. A critical evaluation of the compactibility (σ_0 , MPa) between all L-HPC grades reveals that the compactibility or consolidation behavior of all grades of L-HPC is independent of particle size or HPO content. The similar percolation threshold for compactibility of all L-HPC grades also confirms the consolidation of L-HPC particles is independent of physical or chemical substitutions such as particle size and % of HPO content. This result is consistent with the findings of Queiroz et al. [53], who report that two MCC grades of different physical characteristics show similar compactibility as well as percolation threshold owing to their similar bonding behavior.

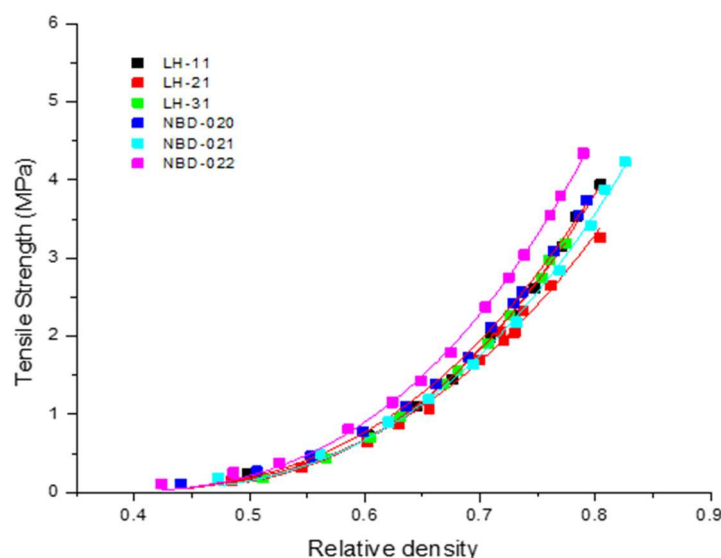


Figure 5. Tensile strength vs. relative density of L-HPC grades as per percolation model (Equation (6)). The results of fitting parameters by nonlinear regression analysis are summarized in Table 5.

A comparative evaluation of compactibility of L-HPC grades with previously reported data of MCC PH 102 ($\sigma_0 = 12.66 \pm 0.24$) using the percolation model ($q = 2.7$) reveals that the compactibility of L-HPC grades is close to the highly compactible MCC PH 102, with NBD-022 showing almost equivalent compactibility (Table 5) [13,31]. Thus, based on the present study, it can be concluded that L-HPC is highly compactible, similar to MCC, and thus L-HPC grades can be applied as a binder in direct compression. The higher R^2 values and adjusted R^2 values, along with low standard error of fitting and root mean square error

(RMSE) values, indicate a good fitting of L-HPC compaction data using the percolation model (Table 5), thus confirming the robustness of the application of percolation model for the estimation of compactibility of all L-HPC grades in the present study.

Table 5. Value of compactibility parameter and percolation threshold of L-HPC grades calculated by percolation model (Equation (6)). All values are reported as parameter \pm standard error of fit.

L-HPC Grade	Compactibility σ_0 , (MPa)	Percolation Threshold (ρ_r) (-)	R ²	Adjusted R ²	Root Mean Square Error (RMSE)
LH-11	10.88 \pm 0.26	0.377 \pm 0.008	0.9976	0.9973	0.07
LH-21	8.91 \pm 0.34	0.350 \pm 0.013	0.9931	0.9924	0.08
LH-31	10.82 \pm 0.15	0.378 \pm 0.004	0.9992	0.9991	0.03
NBD-020	10.55 \pm 0.14	0.355 \pm 0.004	0.9992	0.9991	0.04
NBD-021	9.95 \pm 0.25	0.366 \pm 0.010	0.9973	0.9970	0.08
NBD-022	12.51 \pm 0.21	0.358 \pm 0.005	0.9989	0.9988	0.05

3.4. Disintegration Behavior of L-HPC Grades

Disintegration behavior of the tablet is a complex phenomenon involving various mechanisms such as wicking, swelling, strain recovery, interruption of particle–particle bonds, and heat of interaction [54]. Among them, wicking and swelling are the most widely accepted mechanisms [55]. When disintegrant particles come in contact with water, they swell to a larger extent, usually more than 10 times their original size. In the case of super disintegrants, this could be more than 50–100 times [56]. Due to the swelling of the particles, rapid breakage of the bond between particle occurs, resulting in the disintegration of the tablet. L-HPC has been reported to undergo swelling to a larger extent compared to crospovidone and croscarmellose sodium due to the development of higher swelling pressure, thus causing rapid disintegration of the tablet. However, the phenomenon of water absorption (wicking) and swelling largely depends upon the physical properties as well as the chemical composition of the disintegrant particle [54]. In the present study, to depict the effect of particle size and %HPO content, swelling pressure and water absorption by different grades of L-HPC are studied. As observed in Figure 6, LH-31 shows the lowest water absorption and swelling pressure generated throughout the study. This could be attributed to the small particle size of LH-31 (19.4 μ m) due to which water absorption occurs slowly and thus weak swelling forces are generated. Bele and Derle [57] also reported slow water absorption and weaker swelling of smaller particle disintegrants because of the reduction in intra-particulate porosity, thus reducing the wicking ability and extent of water uptake. Further, the effect of %HPO content of L-HPC grades (NBD-020, NBD-021, and NBD-022) on water absorption and swelling phenomenon has also been elucidated in Figure 7. It was found that NBD-022 having lower HPO content (HPO content = 8.2%) shows the highest swelling pressure and faster water absorption, reaching a plateau within a short period of time, whereas the NBD-020, which has the highest %HPO content (13.8%), shows a slow water absorption and a smaller swelling pressure (Figure 7). This could be attributed to higher hydrophilicity of NBD-020 grade because of the high substitution of the HPO group, due to which absorption of water occurs slowly over a long period time, thus rendering swelling pressure weaker [54,55]. Hence, from the above study, it can be confirmed that particle size and %HPO content of L-HPC grades have significant effects on water absorption and swelling phenomena. As these two mechanisms eventually determine the disintegration time of the tablet, the effect of particle size and %HPO content of L-HPC grades on disintegration behavior of L-HPC tablets was studied using two design matrixes of 3² full-factorial design (Table 2). Along with the physicochemical properties, the porosity or the microstructure of tablets also plays an important role in the wicking of water followed by swelling and finally disintegration of tablet compacts. As porosity largely depends on the compression load applied, the effect of particle size, %HPO content, and compression load on the porosity of L-HPC tablets have also been studied [19].

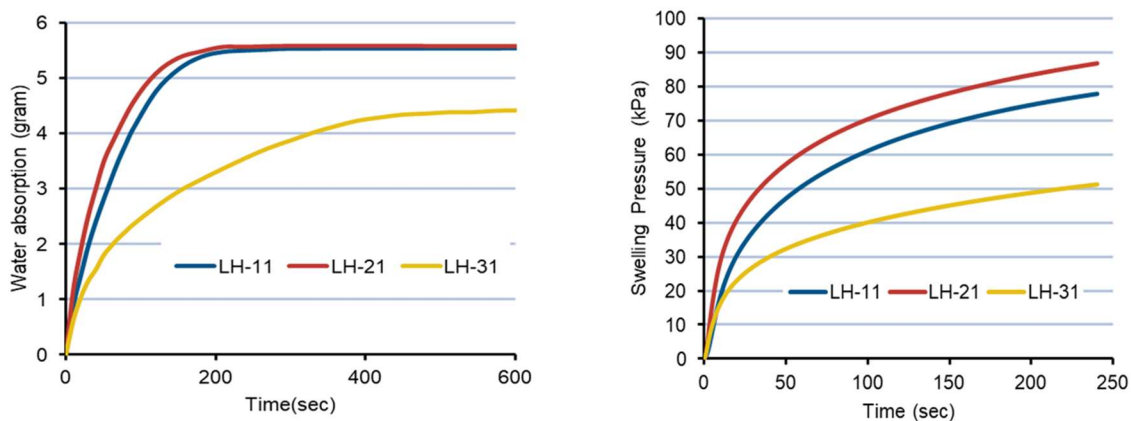


Figure 6. Effect of particle size of different L-HPC grades on water absorption and swelling pressure.

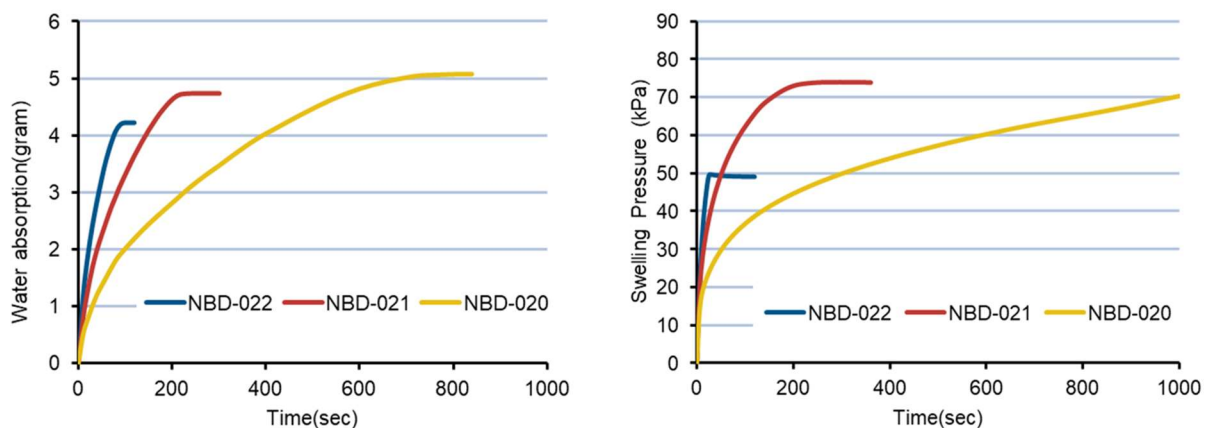


Figure 7. Effect of % hydroxypropyl content (HPO) of different L-HPC grades on water absorption and swelling pressure.

3.4.1. Effect of Particle Size of L-HPC Grades and Compression Load on the Porosity and Disintegration Time of Tablets Using a 3² Full-Factorial Design

The effects of three different particle sizes of L-HPC grades (LH-31, LH-21, and LH-11) and the compression load applied on the porosity of compact, as well as disintegration time along with statistical analysis by ANOVA, are summarized in Table S1 (supplementary materials). The response of independent variables (particle size and compression load) on porosity and disintegration time is plotted in Figure 8. The mean tablet porosity and disintegration time were found to be 27.35% and 716.88 s, respectively (Table S1). The following polynomial equation generated by multiple regression analysis represents the degree of the quantitative effect of particle size (X_1) and compression load (X_2) on porosity and disintegration time.

$$\text{Tablet porosity}(\%) = 27.55 - 0.69X_1 - 8.55X_2 - 0.25X_1X_2 \quad (8)$$

$$\text{Disintegration time}(s) = 843.98 - 441.47X_1 + 610.59X_2 - 310.63X_1X_2 \quad (9)$$

Based on the polynomial equation and statistical data (Table S1), among independent variables, only compression load (X_2) was found to have a statistically significant effect ($p < 0.05$) on tablet porosity, while both particle size (X_1) and compression load (X_2) were found to have a significant effect on disintegration time of the tablet. The quality of the fit of the model, where values of correlation coefficient $R^2 = 0.9822$ and root mean square error RMSE = 1.27 for tablet porosity and $R^2 = 0.9891$ and RMSE = 88.52 for disintegration time, indicate an excellent correlation between observed and predicted values. According to Equations (8) and (9), the positive and negative signs of coefficients of independent

variables indicate the degree of influence on both responses as increasing and decreasing, respectively [19]. Thus, changing the compression load from 25 MPa to 75 MPa causes a significant decrease in the porosity of compact, whereas the particle size does not have a significant effect. The decrease in the porosity of compact with the increase in compression load can be attributed to particles coming closer and undergoing deformation and consolidation. In the case of disintegration time, it was found that changing particle size of L-HPC from 19.4 (LH-31) to 52 μm (LH-11) causes a significant decrease ($p < 0.05$) in disintegration time (Table S1). This could be due to smaller particles size grades of LH-31 exhibiting low swelling pressure, thus having a longer disintegration time (Figure 6). A similar increase in disintegration time with a decrease in particle size of rice starch has been reported by Smallenbroek et al. [58], whereas changing compression load from 25 to 75 MPa causes an increase in disintegration time of L-HPC tablets. This is because the increase in compression load decreases the porosity of the compact due to which the penetration of water media in the compact is reduced, thus resulting in the reduction in the swelling of particles and the increase in disintegration time [19]. Additionally, a significant negative interaction effect ($p < 0.05$) of particle size and compression load on disintegration time was found, indicating that changing particle size and compression load simultaneously decreases the disintegration time of L-HPC tablets significantly.

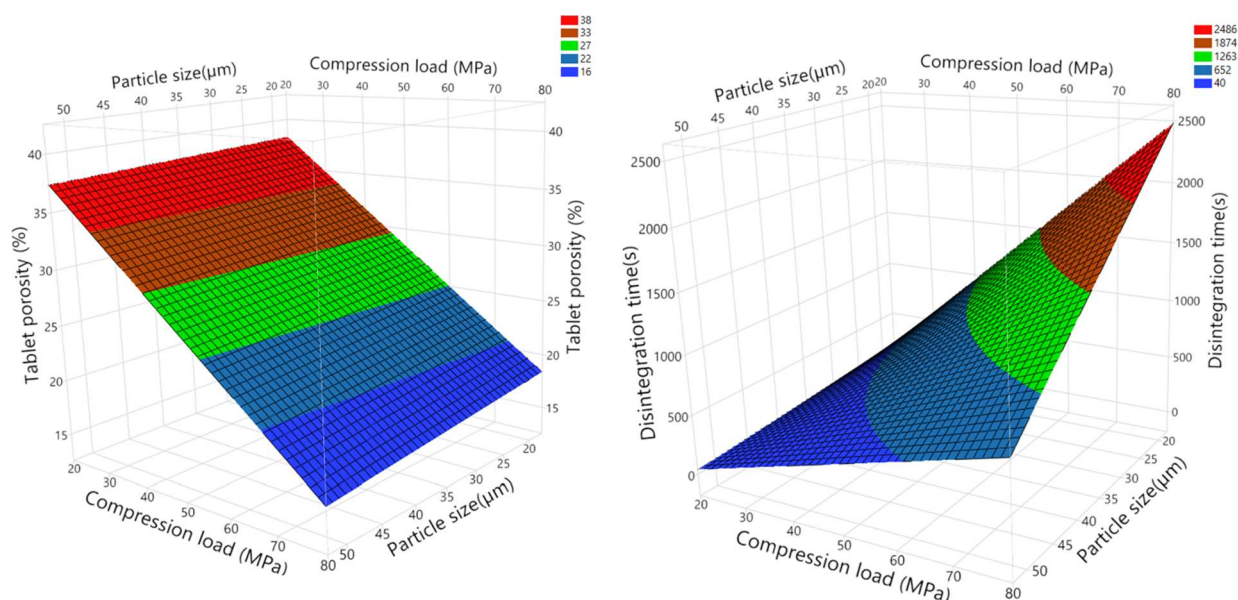


Figure 8. Response surface plot depicting effect of particle size (μm) and compression load (MPa) on tablet porosity (%) and disintegration time(s) of tablets.

3.4.2. Effect of HPO (%) Content of L-HPC Grades and Compression Load on Porosity and Disintegration Time of Tablets Using 3^2 Full-Factorial Design

The statistical analysis of the effect of %HPO content and compression load on porosity and disintegration time has been summarized in Table S2 (Supplementary Materials). The mean tablet porosity and disintegration time were found to be 28.13 % and 242.15 s, respectively. The model was found to be of high quality for disintegration time with higher R^2 and high Adj. R^2 values compared to tablet porosity, which shows low R^2 and Adj. R^2 value. The response plot depicting the effects of %HPO content and compression load on porosity and disintegration time is shown in Figure 9. The polynomial equations indicating the effect of independent variables on porosity and disintegration time are summarized in Equations (10) and (11), respectively.

$$\text{Porosity}(\%) = 28.13 - 0.46X_1 - 9.62X_2 - 0.08X_1X_2 \quad (10)$$

$$\text{Disintegration time}(\text{s}) = 243.38 + 102.50X_1 + 148.47X_2 + 37.25X_1X_2 \quad (11)$$

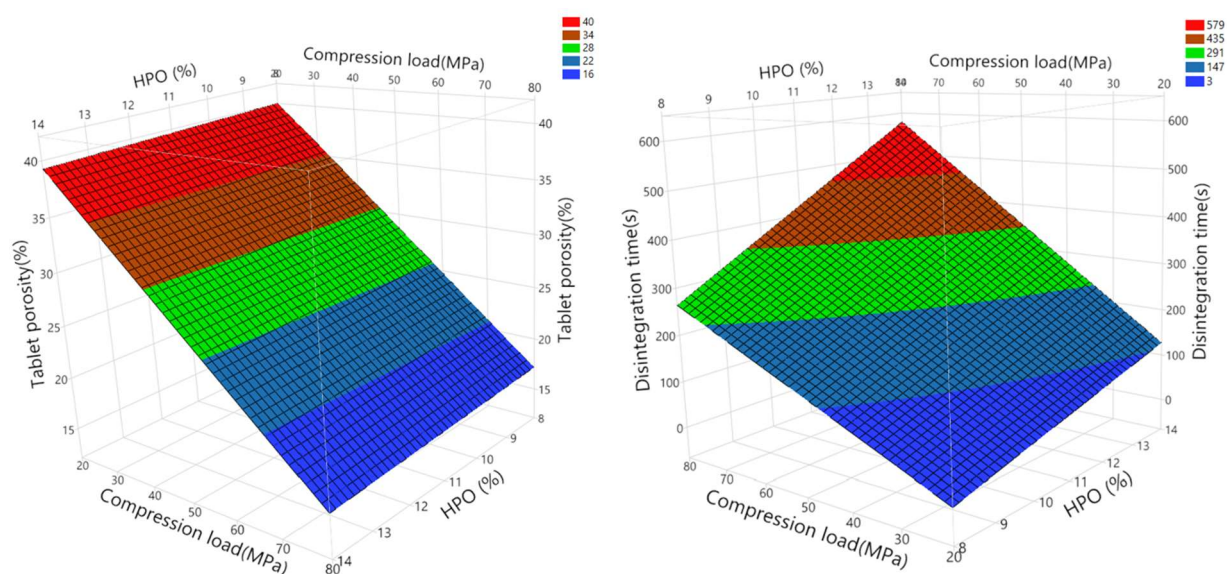


Figure 9. Response surface plot depicting effect of hydroxypropyl (%HPO) content and compression load (MPa) on tablet porosity (%) and disintegration time(s) of tablets.

Based on Equations 10 and 11, as well as ANOVA values (Table S2), it was found that only the compression load has a significant effect on tablet porosity, whereas %HPO content of L-HPC grades does not have a significant effect on the porosity of the compact. The porosity of the compact independent of %HPO content has also been found in our compressibility and compactibility studies (Tables 4 and 5). As evident in Table S2, in the case of disintegration time, both the independent variables, %HPO content and compression load, have a significant effect ($p < 0.05$). Based on Equation (11), it can be observed from the positive sign that increasing the %HPO content (from 8.2% to 13.8%) significantly increases the disintegration time. This could be attributed to the increase in hydrophilicity of the polymer due to the increase in the %HPO content, due to which the swelling efficiency of disintegrant particles decreases (Figure 7), and thus the disintegration time of tablets increases [16,55]. The effect of the increase in hydrophilicity causing an increase in disintegration time of tablets has also been supported by Markl and Zeitler [59] in their disintegration mechanism review. A critical evaluation of the effect of independent variables on the disintegration time from both the design matrixes indicates that %HPO content of L-HPC grades have a lower degree of effect with a lower coefficient value (102.50) compared to the particle size of higher coefficient (441.47). This indicates that although %HPO content has a significant effect ($p < 0.05$) on disintegration time, particle size is more critical for the disintegration of the L-HPC tablets. Thus, careful selection of L-HPC grades should be made during the formulation development of the tablets' dosage form.

Among independent variables, compression load was also found to have a significant effect on disintegration time owing to a decrease in the porosity of the tablet due to an increase in the compression load. Additionally, the interaction effect of %HPO content and compression load on disintegration time was found to be significant ($p < 0.05$), with a positive sign, indicating an increase in disintegration time with a simultaneous increase in both %HPO content and compression load.

4. Conclusions

Delivery of drug at the desired site and desired rate largely depends on the excipients used. Thus, understanding the excipients' functionality and variability is critical for the successful formulation development of the dosage form. In the present study, six different grades of L-HPCs (LH-11, LH-21, LH-31, NBD-020, NBD-021, NBD-022) with different particle sizes and %HPO contents were studied, and their effect on compaction and disintegration behavior were evaluated. An integrated approach to the statistical evaluation

using compaction models and QbD methodology was used to study the variability of L-HPC grades on quality attributes of tablets. It was found that all tested grades of L-HPC are highly compressible, undergoing predominantly plastic deformation. Additionally, it was found that particle size has a large effect on deformation behavior/compressibility of L-HPC, and LH-31 with smaller particles was found to be less compressible compared to other grades of L-HPC such as LH-21 and LH-11. The compactibility of L-HPC was found to be equivalent to microcrystalline cellulose, demonstrating its applicability as a binder. From the 3² full-factorial design, it was found that disintegration time of L-HPC tablets was significantly influenced by particle size and %HPO content, while tablet porosity is largely dependent upon the compression load. It was also found that reducing particle size or increasing %HPO significantly increases the disintegration time due to the decrease in water absorption and swelling pressure. From the DoE study, it was found that particle size of L-HPC grades demonstrates a larger degree of effect compared to %HPO on disintegration time, showing a higher coefficient value. Thus, based on the present study, it can be concluded that variability in L-HPC can have a significant influence on critical quality attributes of tablets such as compaction and disintegration behavior, and thus the selection of the correct grade of L-HPC is critical for successful formulation development.

Supplementary Materials: The following supporting information can be downloaded at: <https://www.mdpi.com/article/10.3390/macromol2010007/s1>, Table S1: Statistical Analysis of effect of particle size of L-HPC grades and compression load on tablet porosity (%) and disintegration time (s); Table S2: Statistical Analysis of effect of % HPO content of L-HPC grades and compression load on tablet porosity (%) and disintegration time (s).

Author Contributions: Conceptualization, S.M.M.; Methodology, S.M.M.; Software, S.M.M.; Validation, S.M.M. and A.S.; Formal Analysis, S.M.M.; Investigation, S.M.M.; Resources, S.M.M. and A.S.; Data Curation, S.M.M.; Writing—Original Draft Preparation, S.M.M.; Writing—Review and Editing, S.M.M. and A.S. All authors have read and agreed to the submitted version of the manuscript.

Funding: This research received no external funding.

Institutional Review Board Statement: Not applicable.

Informed Consent Statement: Not applicable.

Data Availability Statement: The data presented in this study are available in this article or Supplementary Material.

Acknowledgments: We thank Y. Hirama from Shin-Etsu Chemical Co., Ltd. (Tokyo, Japan), for evaluation of swelling pressure and water absorption as well as providing constructive comments and suggestions in the manuscript.

Conflicts of Interest: S.M.M. and A.S. are employees of SE Tylose USA Inc. and SE Tylose GmbH & Co., KG, part of the Shin-Etsu group. The authors alone are responsible for the content and writing of this article.

References

1. Dave, V.S.; Saoji, S.D.; Raut, N.A.; Haware, R.V. Excipient Variability and Its Impact on Dosage Form Functionality. *J. Pharm. Sci.* **2015**, *104*, 906–915. [[CrossRef](#)] [[PubMed](#)]
2. Nakai, Y.; FUKUOKA, E.; NAKAJIMA, S.; HASEGAWA, J. Crystallinity and Physical Characteristics of Microcrystalline Cellulose. *Chem. Pharm. Bull.* **1977**, *25*, 96–101. [[CrossRef](#)]
3. Thoorens, G.; Krier, F.; Leclercq, B.; Carlin, B.; Evrard, B. Microcrystalline Cellulose, a Direct Compression Binder in a Quality by Design Environment—A Review. *Int. J. Pharm.* **2014**, *473*, 64–72. [[CrossRef](#)]
4. Thoorens, G.; Krier, F.; Rozet, E.; Carlin, B.; Evrard, B. Understanding the Impact of Microcrystalline Cellulose Physicochemical Properties on Tabletability. *Int. J. Pharm.* **2015**, *490*, 47–54. [[CrossRef](#)]
5. Krueger, C.; Thommes, M.; Kleinebudde, P. “Mcc Sanaq[®] Burst”—A New Type of Cellulose and Its Suitability to Prepare Fast Disintegrating Pellets. *J. Pharm. Innov.* **2010**, *5*, 45–57. [[CrossRef](#)]
6. Pinakin, P.; Pandey, N.K.; Singh, S.K.; Garg, V. Mcc Sanaq[®] Burst: A Unique Carrier for Formulation of Sublingual Tablets. *Int. J. Pharm. Tech. Res.* **2016**, *9*, 15–22.

7. Pazesh, S.; Persson, A.S.; Alderborn, G. Atypical Compaction Behaviour of Disordered Lactose Explained by a Shift in Type of Compact Fracture Pattern. *Int. J. Pharm. X* **2019**, *1*, 100037.
8. Omar, C.S.; Dhenge, R.M.; Palzer, S.; Hounslow, M.J.; Salman, A.D. Roller Compaction: Effect of Relative Humidity of Lactose Powder. *Eur. J. Pharm. Biopharm.* **2016**, *106*, 26–37. [[CrossRef](#)]
9. Kleinebudde, P. Application of Low Substituted Hydroxypropylcellulose (L-Hpc) in the Production of Pellets Using Extrusion/Spheronization. *Int. J. Pharm.* **1993**, *96*, 119–128. [[CrossRef](#)]
10. EFSA Panel on Food Additives and Nutrient Sources added to Food (ANS); Younes, M.; Aggett, P.; Aguilar, F.; Crebelli, R.; Dusemund, B.; Filipič, M.; Frutos, M.J.; Galtier, P.; Gundert-Remy, U.; et al. Safety of Low-Substituted Hydroxypropyl Cellulose (L-Hpc) to Be Used as a Food Additive in Food Supplements in Tablet Form. *EFSA J.* **2018**, *16*, e05062.
11. ElShaer, A.; Al-Khattawi, A.; Mohammed, A.R.; Warzecha, M.; Lamprou, D.A.; Hassanin, H. Understanding the Compaction Behaviour of Low-Substituted Hpc: Macro, Micro, and Nano-Metric Evaluations. *Pharm. Dev. Technol.* **2018**, *23*, 442–453. [[CrossRef](#)] [[PubMed](#)]
12. Yu, Y.; Zhao, L.; Lin, X.; Wang, Y.; Feng, Y. A Model to Simultaneously Evaluate the Compressibility and Compactibility of a Powder Based on the Compression Ratio. *Int. J. Pharm.* **2020**, *577*, 119023. [[CrossRef](#)] [[PubMed](#)]
13. Mishra, S.M.; Rohera, B.D. Mechanics of Tablet Formation: A Comparative Evaluation of Percolation Theory with Classical Concepts. *Pharm. Dev. Technol.* **2019**, *24*, 954–966. [[CrossRef](#)] [[PubMed](#)]
14. Alvarez-Lorenzo, C.; Gomez-Amoza, J.L.; Martinez-Pacheco, R.; Souto, C.; Concheiro, A. Evaluation of Low-Substituted Hydroxypropylcelluloses (L-Hpcs) as Filler-Binders for Direct Compression. *Int. J. Pharm.* **2000**, *197*, 107–116. [[CrossRef](#)]
15. Schaller, B.E.; Moroney, K.M.; Castro-Dominguez, B.; Cronin, P.; Belen-Girona, J.; Ruane, P.; Croker, D.M.; Walker, G.M. Systematic Development of a High Dosage Formulation to Enable Direct Compression of a Poorly Flowing Api: A Case Study. *Int. J. Pharm.* **2019**, *566*, 615–630. [[CrossRef](#)]
16. Low Substituted Hydroxypropyl Cellulose Nf. 2016. Available online: <https://www.metolose.jp/en/pharmaceutical/l-hpc.html> (accessed on 9 March 2021).
17. Sun, C.C. Quantifying Errors in Tableting Data Analysis Using the Ryshkewitch Equation Due to Inaccurate True Density. *J. Pharm. Sci.* **2005**, *94*, 2061–2068. [[CrossRef](#)]
18. Sun, C.C. A Novel Method for Deriving True Density of Pharmaceutical Solids Including Hydrates and Water-Containing Powders. *J. Pharm. Sci.* **2004**, *93*, 646–653. [[CrossRef](#)]
19. Mishra, S.M.; Rohera, B.D. An Integrated, Quality by Design (Qbd) Approach for Design, Development and Optimization of Orally Disintegrating Tablet Formulation of Carbamazepine. *Pharm. Dev. Technol.* **2017**, *22*, 889–903. [[CrossRef](#)]
20. Mamidi, H.K.; Mishra, S.M.; Rohera, B.D. Determination of Maximum Flowable Liquid-Loading Potential of Neusilin®Us2 and Investigation of Compressibility and Compactibility of Its Liquisolid Blends with Peg (400). *J. Drug Deliv. Sci. Technol.* **2019**, *54*, 101285. [[CrossRef](#)]
21. Tye, C.K.; Sun, C.C.; Amidon, G.E. Evaluation of the Effects of Tableting Speed on the Relationships between Compaction Pressure, Tablet Tensile Strength, and Tablet Solid Fraction. *J. Pharm. Sci.* **2005**, *94*, 465–472. [[CrossRef](#)]
22. Fell, J.T.; Newton, J.M. Determination of Tablet Strength by the Diametral-Compression Test. *J. Pharm. Sci.* **1970**, *59*, 688–691. [[CrossRef](#)]
23. Zhao, N.; Augsburger, L.L. The Influence of Swelling Capacity of Superdisintegrants in Different Ph Media on the Dissolution of Hydrochlorothiazide from Directly Compressed Tablets. *AAPS Pharmscitech* **2005**, *6*, E120–E126. [[CrossRef](#)] [[PubMed](#)]
24. Leuenberger, H. The Compressibility and Compactibility of Powder Systems. *Int. J. Pharm.* **1982**, *12*, 41–55. [[CrossRef](#)]
25. Leuenberger, H.; Rohera, B.D. Fundamentals of Powder Compression. I. The Compactibility and Compressibility of Pharmaceutical Powders. *Pharm. Res.* **1986**, *3*, 12–22. [[CrossRef](#)] [[PubMed](#)]
26. Heckel, R.W. Density-Pressure Relationships in Powder Compaction. *Trans. Metall. Soc. AIME* **1961**, *221*, 671–675.
27. Paul, S.; Sun, C.C. The Suitability of Common Compressibility Equations for Characterizing Plasticity of Diverse Powders. *Int. J. Pharm.* **2017**, *532*, 124–130. [[CrossRef](#)]
28. Kuentz, M.; Leuenberger, H. Pressure Susceptibility of Polymer Tablets as a Critical Property: A Modified Heckel Equation. *J. Pharm. Sci.* **1999**, *88*, 174–179. [[CrossRef](#)]
29. Ryshkewitch, E. Compression Strength of Porous Sintered Alumina and Zirconia. *J. Am. Ceram. Soc.* **1953**, *36*, 65–68. [[CrossRef](#)]
30. van Veen, B.; van der Voort Maarschalk, K.; Bolhuis, G.K.; Frijlink, H.W. Predicting Mechanical Properties of Compacts Containing Two Components. *Powder Technol.* **2004**, *139*, 156–164. [[CrossRef](#)]
31. Mishra, S.M. Investigation of Compaction Behavior of Pharmaceutical Powders: An Elucidation Based on Percolation Theory. Ph.D. Thesis, Saint John’s University, New York, NY, USA, 2019.
32. Leuenberger, H.; Leu, R. Formation of a Tablet: A Site and Bond Percolation Phenomenon. *J. Pharm. Sci.* **1992**, *81*, 976–982. [[CrossRef](#)]
33. Guyon, E.; Roux, S.; Hansen, A.; Bideau, D.; Troadec, J.P.; Crapo, H. Non-Local and Non-Linear Problems in the Mechanics of Disordered Systems: Application to Granular Media and Rigidity Problems. *Rep. Prog. Phys.* **1990**, *53*, 373. [[CrossRef](#)]
34. Kuentz, M.; Leuenberger, H. A New Theoretical Approach to Tablet Strength of a Binary Mixture Consisting of a Well and a Poorly Compactable Substance. *Eur. J. Pharm. Biopharm.* **2000**, *49*, 151–159. [[CrossRef](#)]
35. Bates, D.M.; Watts, D.G. *Nonlinear Regression Analysis and Its Applications*; Wiley: New York, NY, USA, 1988; Volume 2.

36. Pabari, R.M.; Ramtoola, Z. Application of Face Centred Central Composite Design to Optimise Compression Force and Tablet Diameter for the Formulation of Mechanically Strong and Fast Disintegrating Orodispersible Tablets. *Int. J. Pharm.* **2012**, *430*, 18–25. [[CrossRef](#)] [[PubMed](#)]
37. Solaiman, A.; Suliman, A.S.; Shinde, S.; Naz, S.; Elkordy, A.A. Application of General Multilevel Factorial Design with Formulation of Fast Disintegrating Tablets Containing Croscaremellose Sodium and Disintequick Mcc-25. *Int. J. Pharm.* **2016**, *501*, 87–95. [[CrossRef](#)]
38. Jivraj, M.; Martini, L.G.; Thomson, C.M. An Overview of the Different Excipients Useful for the Direct Compression of Tablets. *Pharm. Sci. Technol. Today* **2000**, *3*, 58–63. [[CrossRef](#)]
39. Mattsson, S. Pharmaceutical Binders and Their Function in Directly Compressed Tablets: Mechanistic Studies on the Effect of Dry Binders on Mechanical Strength, Pore Structure and Disintegration of Tablets. Ph.D. Thesis, Acta Universitatis Upsaliensis, Uppsala, Sweden, 2000.
40. Osei-Yeboah, F.; Chang, S.Y.; Sun, C.C. A Critical Examination of the Phenomenon of Bonding Area-Bonding Strength Interplay in Powder Tableting. *Pharm. Res.* **2016**, *33*, 1126–1132. [[CrossRef](#)]
41. Olsson, H.; Mattsson, S.; Nyström, C. Evaluation of the Effect of Addition of Polyethylene Glycols of Differing Molecular Weights on the Mechanical Strength of Sodium Chloride and Sodium Bicarbonate Tablets. *Int. J. Pharm.* **1998**, *171*, 31–44. [[CrossRef](#)]
42. Reus-Medina, M.; Lanz, M.; Kumar, V.; Leuenberger, H. Comparative Evaluation of the Powder Properties and Compression Behaviour of a New Cellulose-Based Direct Compression Excipient and Avicel Ph-102. *J. Pharm. Pharmacol.* **2004**, *56*, 951–956. [[CrossRef](#)]
43. Ghori, M.U.; Conway, B.R. Powder Compaction: Compression Properties of Cellulose Ethers. *Br. J. Pharm.* **2016**, *1*, 19–29. [[CrossRef](#)]
44. Sano, S.; Iwao, Y.; Noguchi, S.; Kimura, S.; Itai, S. Design and Evaluation of Microwave-Treated Orally Disintegrating Tablets Containing Polymeric Disintegrant and Mannitol. *Int. J. Pharm.* **2013**, *448*, 132–141. [[CrossRef](#)]
45. Roberts, R.J.; Rowe, R.C. The Effect of the Relationship between Punch Velocity and Particle Size on the Compaction Behaviour of Materials with Varying Deformation Mechanisms. *J. Pharm. Pharmacol.* **1986**, *38*, 567–571. [[CrossRef](#)] [[PubMed](#)]
46. Müller, F.S. Modified Celluloses as Multifunctional Excipients in Rapidly Dissolving Immediate Release Tablets. Ph.D. Thesis, University of Basel, Basel, Switzerland, 2008.
47. Ghori, M.U.; Grover, L.M.; Asare-Addo, K.; Smith, A.M.; Conway, B.R. Evaluating the Swelling, Erosion, and Compaction Properties of Cellulose Ethers. *Pharm. Dev. Technol.* **2018**, *23*, 183–197. [[CrossRef](#)] [[PubMed](#)]
48. Riepma, K.A.; Lerk, C.F.; De Boer, A.H.; Bolhuis, G.K.; Kussendrager, K.D. Consolidation and Compaction of Powder Mixtures. I. Binary Mixtures of Same Particle Size Fractions of Different Types of Crystalline Lactose. *Int. J. Pharm.* **1990**, *66*, 47–52. [[CrossRef](#)]
49. Wu, C.-Y.; Best, S.M.; Bentham, A.C.; Hancock, B.C.; Bonfield, W. Predicting the tensile strength of compacted multi-component mixtures of pharmaceutical powders. *Pharm. Res.* **2006**, *23*, 1898–1905. [[CrossRef](#)] [[PubMed](#)]
50. Leane, M.; Pitt, K.; Reynolds, G.; Manufacturing Classification System (MCS) Working Group. A Proposal for a Drug Product Manufacturing Classification System (Mcs) for Oral Solid Dosage Forms. *Pharm. Dev. Technol.* **2015**, *20*, 12–21. [[CrossRef](#)]
51. Wu, C.Y.; Best, S.M.; Bentham, A.C.; Hancock, B.C.; Bonfield, W. A Simple Predictive Model for the Tensile Strength of Binary Tablets. *Eur. J. Pharm. Sci.* **2005**, *25*, 331–336. [[CrossRef](#)]
52. Sun, C.C. Decoding Powder Tableability: Roles of Particle Adhesion and Plasticity. *J. Adhes. Sci. Technol.* **2011**, *25*, 483–499. [[CrossRef](#)]
53. Queiroz, A.L.; Faisal, W.; Devine, K.; Garvie-Cook, H.; Vucen, S.; Crean, A.M. The Application of Percolation Threshold Theory to Predict Compaction Behaviour of Pharmaceutical Powder Blends. *Powder Technol.* **2019**, *354*, 188–198. [[CrossRef](#)]
54. Desai, P.M.; Liew, C.V.; Heng, P.W. Review of Disintegrants and the Disintegration Phenomena. *J. Pharm. Sci.* **2016**, *105*, 2545–2555. [[CrossRef](#)]
55. Berardi, A.; Bisharat, L.; Quodbach, J.; Rahim, S.A.; Perinelli, D.R.; Cespi, M. Advancing the Understanding of the Tablet Disintegration Phenomenon—an Update on Recent Studies. *Int. J. Pharm.* **2021**, *598*, 120390. [[CrossRef](#)]
56. Zhao, N.; Augsburg, L.L. Functionality Comparison of 3 Classes of Superdisintegrants in Promoting Aspirin Tablet Disintegration and Dissolution. *AAPS Pharmscitech* **2005**, *6*, E634–E640. [[CrossRef](#)] [[PubMed](#)]
57. Bele, M.H.; Derle, D.V. Mechanism of Disintegrant Action of Polacrillin Potassium: Swelling or Wicking? *Acta Pharm. Sin. B* **2012**, *2*, 70–76. [[CrossRef](#)]
58. Smallenbroek, A.J.; Bolhuis, G.K.; Lerk, C.F. The Effect of Particle Size of Disintegrants on the Disintegration of Tablets. *Pharm. Weekbl.* **1981**, *3*, 1048–1051. [[CrossRef](#)]
59. Markl, D.; Zeitler, J.A. A Review of Disintegration Mechanisms and Measurement Techniques. *Pharm. Res.* **2017**, *34*, 890–917. [[CrossRef](#)]